Journal of Hazardous Materials 184 (2010) 612–619

Contents lists available at ScienceDirect

Journal of Hazardous Materials

journal homepage: www.elsevier.com/locate/jhazmat

Hydrothermal synthesis of TiO_2 hollow microspheres for the photocatalytic degradation of 4-chloronitrobenzene

Miaomiao Ye[a,b], Zhonglin Chen[a,*], Wenshou Wang[c], Jimin Shen[a], Jun Ma[a]

[a] State Key Laboratory of Urban Water Resource and Environment, Harbin Institute of Technology, Harbin 150090, PR China
[b] Institute of Municipal Engineering, Zhejiang University, Hangzhou, 310058, PR China
[c] School of Materials Science and Engineering, Harbin Institute of Technology, Harbin 150001, PR China

ARTICLE INFO

Article history:
Received 13 May 2010
Received in revised form 18 August 2010
Accepted 20 August 2010
Available online 27 August 2010

Keywords:
TiO_2 hollow microspheres
Hydrothermal method
Photocatalysis
4-Chloronitrobenzene
Recycling

ABSTRACT

TiO_2 hollow microspheres were synthesized by a simple hydrothermal method followed by calcination at different temperatures ranging from 400 to 800 °C. The prepared samples were characterized by XRD, SEM, TEM, SAED, HRTEM, N_2 adsorption, and UV–vis spectroscopy. The photocatalytic activities of the hollow microspheres were evaluated by photocatalytic decomposition of 4-chloronitrobenzene (4-CNB). Results showed that the TiO_2 hollow microspheres, which had an average external diameter of 1.75 μm, were composed of numerous TiO_2 nanoparticles. Photocatalysis experiments indicated that the TiO_2 hollow microspheres calcined at 500 °C exhibited the highest photocatalytic activity, which was nearly 2 and 1.5 times higher than that of the uncalcined sample and Degussa P25, respectively. The catalyst crystallinity, catalyst dosage and 4-CNB concentration were found to have a significant impact on the degradation efficiency whereas solution pH has relatively less effect. The removal of total organic carbon (TOC) and formation of chloride, nitrate (V) anions were monitored to follow the mineralization process of 4-CNB. In addition, it was demonstrated that these TiO_2 hollow microspheres could be recycled easily without decreasing their photocatalytic activities.

1. Introduction

The widespread use of 4-chloronitrobenzene (4-CNB) in the manufacture of pesticides, dyes, pharmaceuticals, photographic chemicals, antioxidants and other industrial chemicals unavoidably results in its release into the aquatic environment [1–3]. It is known that 4-CNB is toxic and non-biodegradable, and that it can cause methemoglobinemia and/or anemia in humans and animals [4]. Further, 4-CNB is weakly mutagenic in the Ames test and shows carcinogenic activity in mice [5]. Considering that 4-CNB is a potentially harmful compound to humans, 4-CNB in wastewater must be removed or decomposed before the wastewater is discharged. Heterogeneous photocatalysis using semiconducting oxide catalysts is an efficient method for the elimination of organic pollutants [6–8]. Nanosized TiO_2 is one of the most popular photocatalysts among the semiconductors being studied due to its favorable characteristics, e.g. low cost, good chemical stability and non-toxicity [9,10]. However, in a practical photocatalytic process, it is very difficult to separate and recover these finely powdered photocatalysts from solution after the reaction. In addition, TiO_2 nanoparticles often show lower efficiencies owing to aggregation problems [11]. Nanocrystalline TiO_2 immobilized on supporting materials can improve the efficiency of separation. Unfortunately, it usually decreases the overall photocatalytic activity due to lowering of the surface-to-volume ratio [12]. In some case, TiO_2 nanoparticles may easily detach from the support, making their complete recovery from the treated solution difficult.

Recently, great efforts have been devoted to achieve a kind of TiO_2-based photocatalyst with high photocatalytic activity and easy recovery. Microspheres with hollow structures have attracted significant interest owing to its high surface-to-volume ratios, good surface permeability, and great light-harvesting capacity for the improvement of photocatalytic activity and the large diameter for the enhancement of separation efficiency [13–19]. For instance, Liu and et al. [20] described a low-temperature hydrothermal method to fabricate porous TiO_2 hollow aggregates with high photocatalytic activity. Lu et al. [21] declared that the photocatalytic activity can be significantly influenced by the tunable chamber structure of the TiO_2 hollow spheres. Yu et al. [22] reported a one-pot approach for nanoporous titania hollow microspheres with high photocatalytic activity due to the hollow structure. Xie et al. [23] reported the fabrication of TiO_2 hollow microspheres via a hydrothermal method using potassium titanium oxalate as titanium source, however, the photocatalytic activity was lower owing to the rutile phase. Herein, we have modified the synthesis route of Xie et al. by tuning the dosage of hydrochloric acid and increasing the reaction time, and

* Corresponding author. Tel.: +86 451 86283028; fax: +86 451 86283028.
E-mail addresses: zhonglinchen@263.net, zhonglinchen@hit.edu.cn (Z. Chen).

0304-3894/$ – see front matter © 2010 Elsevier B.V. All rights reserved.
doi:10.1016/j.jhazmat.2010.08.080

then the as-prepared sample was calcined at different temperatures range from 400 to 800 °C for 2 h. The photocatalytic activities of the TiO_2 hollow microspheres before and after calcination were evaluated by photocatalytic degradation of 4-chloronitrobenzene. Moreover, parameters affecting the photocatalytic process such as catalyst crystallinity, concentration of titania, 4-CNB concentration and initial solution pH were investigated. Finally, the stability of the TiO_2 hollow microspheres calcined at 500 °C was monitored by following the evolution of their photocatalytic activity during six cycles of use.

2. Experimental

2.1. Synthesis of TiO_2 hollow microspheres

All chemicals were of analytical grade and were used without further purification. In a typical synthesis, 1.4 g of potassium titanium oxalate (PTO) was dissolved in 30 mL deionized water, followed by the addition of 30 mL 30% H_2O_2 and 0.8 mL of 37% HCl. The solution was then transferred to a 100 mL Teflon-lined autoclave. The hydrothermal synthesis was conducted at 150 °C for 24 h, and allowed to cool to room temperature naturally. The white precipitates were collected by means of centrifugation, washed several times with deionized water and ethanol, then dried in a vacuum at 60 °C for 8 h and calcined in air at 400, 500, 600 and 800 °C for 2 h.

2.2. Characterization

The crystalline structures of the samples were evaluated by X-ray diffraction (XRD) analyses, carried out on a Rigaku D/max-rA diffractometer with Cu Kα radiation (λ = 1.5405 Å). The size and morphology of the microstructures were analyzed using a Philips ESEM XL30 scanning electron microscope (SEM) equipped with a field-emission gun operated at 10 kV and a Philips Tecnai 12 transmission electron microscope (TEM) at 120 kV. High-resolution transmission electron microscope (HRTEM) images were recorded on a FEI Tecnai F30 microscope, operated at 300 kV. The porosity of the products was measured by the nitrogen adsorption–desorption isotherm and Barrett–Joyner–Halenda (BJH) methods on a Micromeritics ASAP 2020 M accelerated surface area and porosimetry system. Their UV–vis absorption diffuse reflectance spectra were measured on a TU–1901 spectrophotometer equipped with a labsphere diffuse reflectance accessory. The concentration of the Ti^{4+} dissolved in the solution was determined by using a PerkinElmer inductively coupled plasma optical emission spectrometer (ICP–OES) Optima 5300 DV.

2.3. Measurement of photocatalytic activity

Photocatalytic reactions for degradation of 4-CNB were carried out in a Pyrex cylindrical batch photoreactor (4 cm internal diameter with a total volume of 0.5 L, as shown in our previous work [3]), containing 400 mL reaction slurry. Agitation was provided by magnetic stirrer. The initial solution pH range from 2.24 to 10.20 was adjusted by adding sodium hydroxide or perchloric acid. The aqueous slurry, prepared with a given amount of catalyst (0.1–1.0 g/L) and 4-CNB in concentration of (0.1×10^{-5} to 5.0×10^{-5} mol/L), was stirred in the dark for 30 min to ensure that the 4-CNB was adsorbed to saturation on the catalysts. A 10 W UV lamp (254 nm, GPH212T5L/4, Germany), immersed within the suspension, was used as UV radiation source. The average light intensity striking on the surface of the reaction solution was about 2.6 mW/cm^2. It was surrounded by a quartz jacket to cut-off any radiation with wavelength below 254 nm. The suspension temperature was 20 ± 1 °C for each run. For recycling of use the catalysts, after the TiO_2 hollow spheres were separated from solution by filtration, we removed the clear upper solution, then redispersed the catalysts in 4-CNB solution (400 mL) by sonication for another cycling use.

The concentration of 4-CNB was determined by HPLC (Thermo, Finnigan, USA) provided with a UV–vis detector. A 4.6 cm × 150 mm 5 μm ASB–C_{18} column (Agele Inc., USA) was used. The analysis was carried out isocratically with an 80/20 (v/v) methanol/water mobile phase and the flow rate was set at 1.0 mL/min. The total organic carbon (TOC) was analyzed by means of TOC analyzer (TOC-VCPH, Shimadzu, Japan).

The quantitative determination of the anions present in the reaction mixture during the runs was carried out by using an ionic chromatograph (Dionex DX120) equipped with an ION PAC AG11 AS11 column. Condition: eluant, 30 mM, potassium hydroxide; eluant source, EG40; flow rate, 1.2 mL/min; injection, 10 μL; detection, supressed conductivity ASRS*-ULTRA recycle mode; temperature, 30 °C; run time, 10 min.

3. Results and discussion

3.1. Characterization of TiO_2 hollow microspheres

The morphologies and microstructures of the hollow microspheres were characterized by scanning electron microscopy (SEM). Fig. 1a shows a low-magnification SEM image of the uncalcined sample, which performs that the product consisted of large-scale hollow microspheres. The average external diameter of the hollow microspheres was 1.75 μm, as observed by measuring 100 microspheres (as shown in Fig. 1e). A high-magnification SEM image (Fig. 1b) revealed that the shell of the microsphere was composed of numerous nanoparticles. Moreover, the average shell thickness of the hollow microspheres was about 175 nm. After being calcined at 500 °C for 2 h, the morphology and the mean external diameter of the hollow microspheres remained unchanged (as shown in Fig. 1c, d and f), indicating that they possessed excellent thermal stability.

The structure of the TiO_2 hollow microspheres was further studied by transmission electron microscope (TEM) and selected area electron diffraction (SAED) pattern (see Fig. 2a and b). It is clear that the microsphere was hollow with an external diameter of about 1.70 μm, which was in agreement with the SEM observation. The SAED pattern taken from the fringe part of the hollow microsphere indicated that the microsphere was polycrystalline, because it was composed of many nanoparticles. A high-resolution transmission electron microcopy (HRTEM) image in Fig. 2c shows that the space of fringe image was 0.35 nm, corresponding to the distance between (1 0 1) crystal plane of anatase TiO_2.

The XRD patterns of the synthesized TiO_2 hollow microspheres before and after calcination are shown in Fig. 3. Before calcination, the strong and sharp diffraction peaks indicated that the product was highly crystalline. All diffraction peaks of uncalcined and calcined samples can be indexed perfectly to the anatase phase of TiO_2 (JCPDS 21-1272). No characteristic peaks of other impurities were detected in the XRD patterns, indicating that the TiO_2 hollow microspheres calcined at 400–800 °C did not change phase. Noticeably, the anatase structure of the hollow microspheres was maintained even after calcination at 800 °C for 2 h. The same results were obtained by Xu and co-workers [24], who synthesized TiO_2 cuboids that can exist as a pure anatase phase even after calcination up to temperatures as high as 800 °C. According to the Scherrer equation, the average crystal size of the uncalcined TiO_2 hollow microspheres is ca. 6.5 nm (as shown in Table 1). From our data, we can see that there was a small increase in the average crystal size after calcination over the whole temperature range of 400–800 °C.

The effects of calcination temperatures on the pore structure and surface area of the prepared samples were investigated by mea-

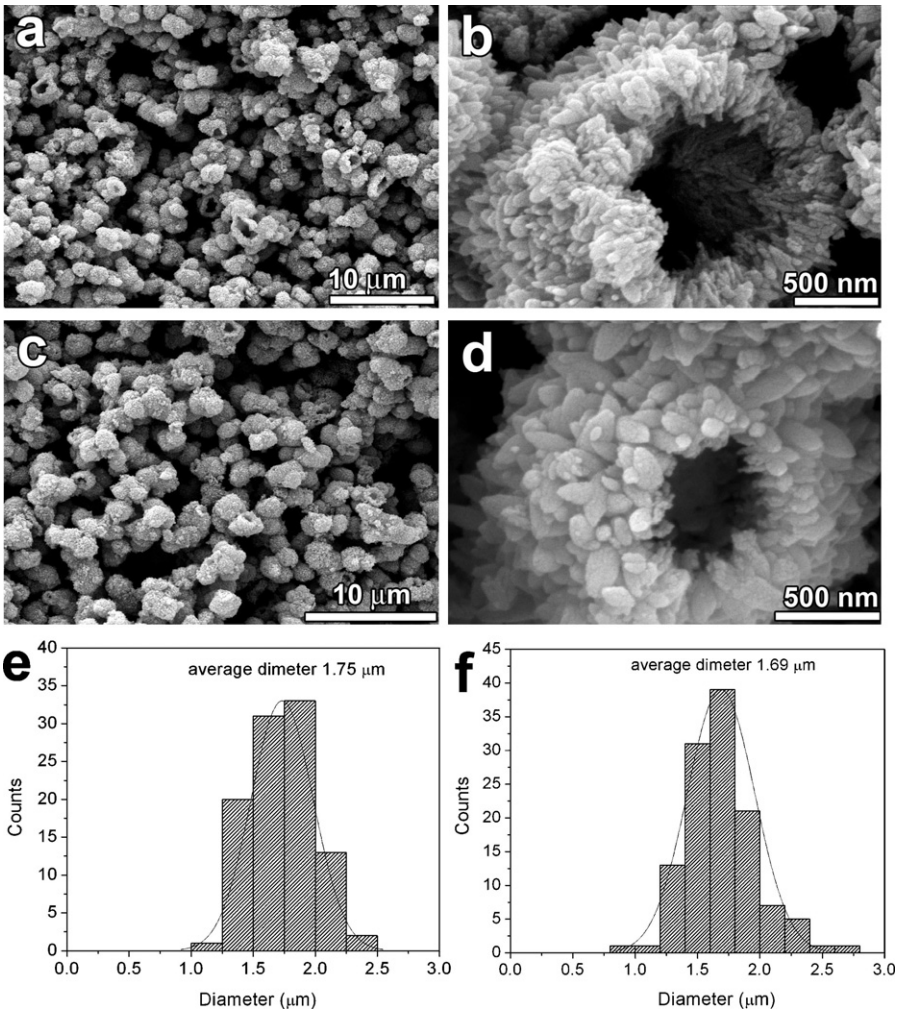

Fig. 1. SEM images of (a) and (b) the uncalcined TiO_2 hollow microspheres and (c) and (d) the TiO_2 hollow microspheres calcined at 500 °C; (e) and (f) size distribution calculated from (a) and (c), respectively.

suring the nitrogen adsorption–desorption isotherm. Fig. 4a shows the nitrogen adsorption–desorption isotherms of the TiO_2 hollow microspheres before and after calcination. Before calcination, the isotherms were of the typical type IV pattern with distinct H_2 and H_3 hysteretic loops in the range of 0.4–0.9P/P_0 and 0.9–1.0P/P_0, respectively, indicating the existence of ink-bottle- and slit-shaped pores according to the IUPAC classification [25]. It is believed that this bimodal distribution of pore sizes results from having pores with two different origins: the smaller mesopores are related to interstices between primary crystallites, whereas the larger ones are associated with secondary interaggregated [16]. Such bimodal pores are beneficial to the enhancement of photocatalytic performance due to more surface active sites for the adsorption of reactants molecules, faster diffusion of various reactants and byproducts, and enhanced harvesting of exciting light by multiple scattering within the porous framework [26–28]. With increasing calcination temperature, the hysteresis loops shifted to a higher relative pressure (P/P_0) range and the area of the hysteresis loops gradually became smaller. This indicated that the average pore size increased and the pore volume decreased [29]. The corresponding pore-size distribution of the TiO_2 hollow microspheres (see Fig. 4b) was determined using the Barrett–Joyner–Halenda (BJH) method

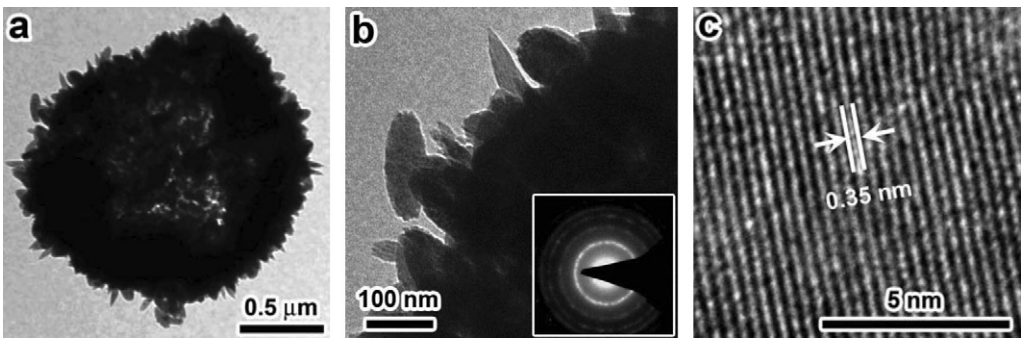

Fig. 2. (a) and (b) TEM images of the uncalcined TiO_2 hollow microspheres; (c) HRTEM image of the selected nanoparticle. Inset: SAED pattern.

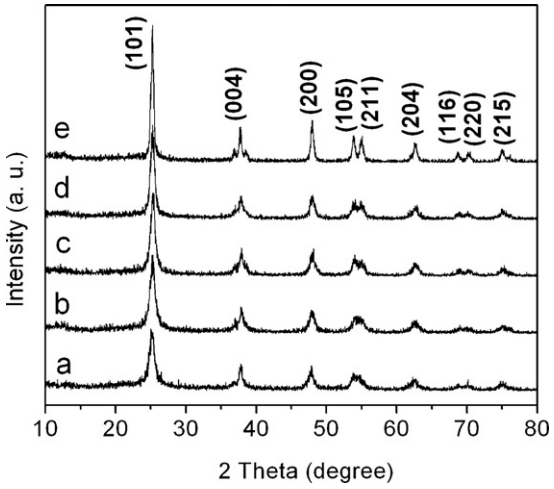

Fig. 3. XRD patterns of the synthesized TiO_2 hollow microspheres (a) before and after calcination at (b) 400 °C, (c) 500 °C, (d) 600 °C, (e) 800 °C for 2 h.

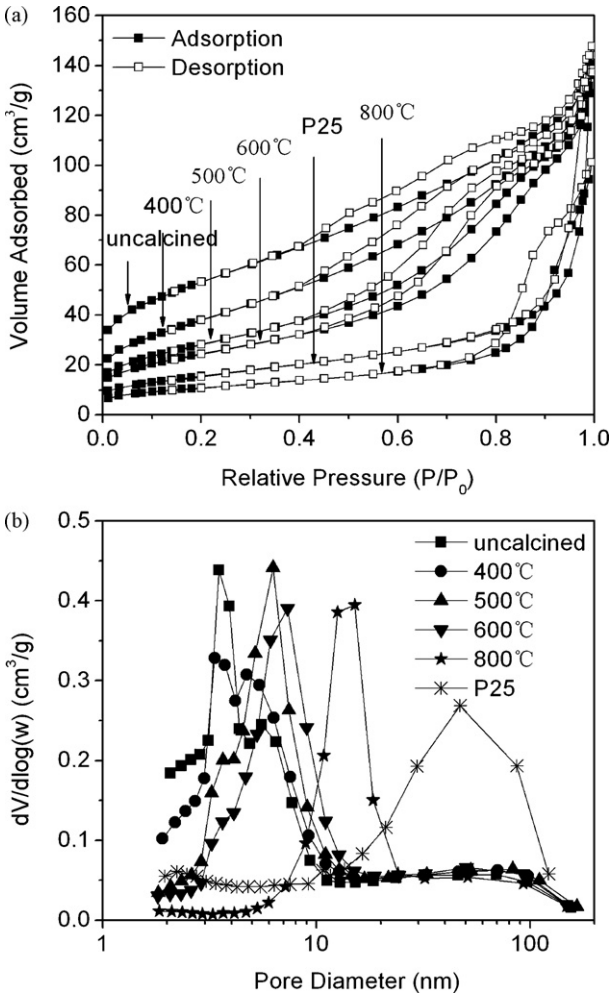

Fig. 4. (a) Nitrogen adsorption–desorption isotherm and (b) BJH pore-size distribution curve of the TiO_2 hollow microspheres before and after calcination.

from the desorption branch of the isotherm. Before calcination, the TiO_2 microspheres contained micropores, mesopores and macropores with an average pore diameter of 5.2 nm. The BET surface area and pore volume of the TiO_2 hollow microspheres were 190.9 m^2/g and 0.1992 cm^3/g, respectively. After calcination the pore volume (especially the micropore volume) of the calcined samples decreased drastically due to the collapse of small pores during calcination. Data concerning the BET surface area, pore volume and average pore size of the TiO_2 hollow microspheres before and after calcination are presented in Table 1. Obviously, the increase in calcination temperature led to a reduction in the BET surface area and total pore volume while increasing the average pore size. Moreover, the value of the BET surface area and total pore volume of the samples calcined at 400–600 °C were much higher than those of Degussa P25. The larger surface area and pore volume are beneficial to offer more active adsorption sites and photocatalytic reaction centers [30], thus improving the photocatalytic activity.

The optical band gaps of the TiO_2 hollow microspheres before and after calcination were studied by the UV–vis optical absorbance spectrum. The relationship between the absorption coefficient (α) and the photon energy ($h\nu$) can be written as shown in Eq. (1) [31]:

$$(\alpha h\nu)^n = B(E - E_g) \quad (1)$$

where B is the constant related to the effective masses associated with the valence and conduction bands, $E = h\nu$ is the photon energy, E_g is the band gap energy, and $n = 1/2$ or 2, depending on whether the transition is indirect or direct. Fig. 5 shows the absorption spectrum of the TiO_2 hollow microspheres before and after calcination. The inset shows the plots of $(\alpha h\nu)^2$ versus the $(h\nu)$ at each calcination temperature. The band gap energy (E_g) for the samples can be calculated by extrapolating the linear portion of $(\alpha h\nu)^2$ versus the $(h\nu)$ plot to $\alpha = 0$. On the basis of these results, the optical band gaps for the samples were 3.37, 3.36, 3.35, 3.37 and 3.36 eV, respectively, which are all close to that of anatase TiO_2 nanoparticles of 5–10 nm (3.36 eV) [32], but higher than that of Degussa P25 (3.28 eV). The obvious blueshift of the optical band gap might be the result of the smaller average crystal size of the TiO_2 microspheres. This is the so-called quantum-size effect. This is accordance with Liu et al. [20] and Zhang et al. [33], who synthesized TiO_2 hollow aggregates and TiO_2 solid spheres with optical band gaps of 3.36 and 3.68 eV, respectively.

Table 1
Effects of calcination temperature on physical properties and apparent rate constants of TiO_2 hollow microspheres.

Temperature (°C)	Anatase/rutile (%)	Crystallite size[a] (nm)	BET surface area (m^2/g)	Total pore volume[b] (cm^3/g)	Pore diameter (nm)	Band gap energy[c] (eV)	Apparent rate constant (min^{-1})
Uncalcined	100	6.5	190.9	0.1992	5.2	3.37	0.05606
400	100	9.0	139.6	0.1906	5.5	3.36	0.08314
500	100	11.2	102.9	0.1841	6.6	3.35	0.10590
600	100	11.7	89.6	0.1795	7.6	3.37	0.07851
800	100	18.6	39.3	0.1272	14.2	3.36	0.05081
Degussa P25	80/20	28.0	56.5	0.1136	14.9	3.28	0.07309

[a] Average crystallite sizes of TiO_2 hollow microspheres before and after calcination were determined by XRD using Scherrer equation.
[b] Pore volume was determined by nitrogen adsorption volume of pores less than 100 nm width at $P/P_0 = 0.97$.
[c] Band gap energy was determined by UV–vis optical absorbance spectrum using the equation of $(\alpha h\nu)^n = B(E - E_g)$.

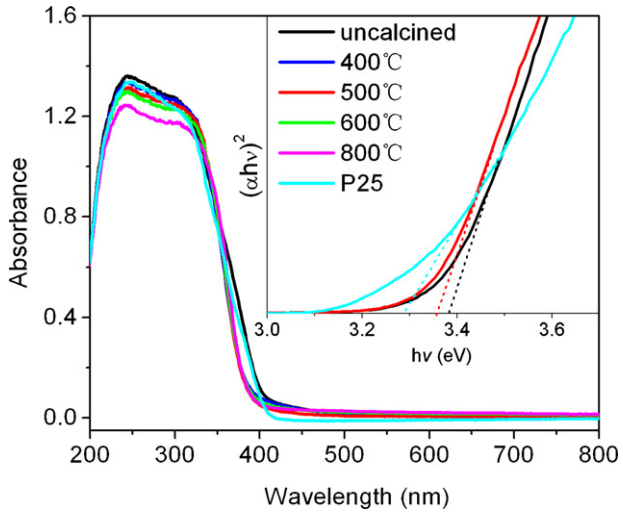

Fig. 5. UV–vis absorbance spectra of the TiO_2 hollow microspheres before and after calcination. The inset shows the plot of $(\alpha h\nu)^2$ versus the $(h\nu)$.

3.2. Photocatalytic degradation of 4-CNB

3.2.1. Effect of calcination temperature

The effect of calcination temperatures on photocatalytic activities of the TiO_2 hollow microspheres is shown in Fig. 6. The calcination temperatures have a significant influence on the photocatalytic activity of the TiO_2 hollow microspheres. We can see from Fig. 6a that the photocatalytic degradation of 4-CNB followed pseudo first order kinetics, and the photocatalytic reaction can be described simply by $dC/dt = -kc$, or $\ln(C_0/C) = kt$, where C and C_0 are the actual and initial concentration of 4-CNB, and k is the apparent degradation rate constant. Before calcination, the photocatalytic activity of the TiO_2 hollow microspheres was poor due to the relatively poor crystallization. The activities of the modified titania hollow spheres and the reported one can be compared by measuring their apparent degradation rate constants (k) since both of the reactions followed pseudo first order kinetics. The k value for the uncalcined sample was 0.05606 min^{-1}, which was slightly higher than that of the reported one (0.05154 min^{-1}, calculated from Fig. 4b, in reference [23]). With increasing calcination temperature, the photocatalytic activity of the microspheres increased due to enhancement of the crystallization. The highest photocatalytic activity was observed at 500 °C and the k value reached 0.1059 min^{-1}, which is about 2 and 1.5 times higher than that of the uncalcined sample and Degussa P25, respectively (as shown in Table 1). With a further increase in calcination temperature to 800 °C, the k value decreased due to the decrease in BET surface area. Generally speaking, the photocatalytic activity of TiO_2 is influenced by many factors including crystal structure, crystal size, surface-to-volume ratio and optical band gap. In our experiment, the TiO_2 hollow microspheres before and after calcination were all in anatase phase, and the optical band gap were almost the same. Therefore, the observation that the highest photocatalytic activity of the TiO_2 hollow microspheres occurred in those calcined at 500 °C might be explained by the enhancement of anatase crystallization and increase in surface area resulting from calcination at this temperature relative to those in samples calcined at 400 and 600 °C [34]. Furthermore, the photocatalytic activities of the samples calcined at various temperatures over the range 400–600 °C were much higher than that of Degussa P25 due to their smaller crystal sizes, lager surface areas and pore volumes as well as better light scattering [35,36].

3.2.2. Effect of reaction conditions

The initial concentration of 4-CNB range from 0.1×10^{-5} to 5.0×10^{-5} mol/L was used for observing the effect of varying 4-CNB concentration on its degradation rate, the results are depicted in Fig. 7. It is clear that the lower the 4-CNB concentration, the higher the efficiency of 4-CNB decomposition. The apparent rate constant values are calculated to be 0.1682, 0.1408, 0.1059, and 0.06468 and 0.03748 min^{-1} with 4-CNB concentration of 0.1×10^{-5}, 0.5×10^{-5}, 1.0×10^{-5}, 2.5×10^{-5}, and 5.0×10^{-5} mol/L, respectively. The presumed reason is that at high 4-CNB concentrations the generation of •OH radicals on the surface of titania hollow spheres is reduced since the active sites are covered by the 4-CNB molecule [7]. Furthermore, at a high 4-CNB concentration, a part of UV light may be absorbed by the 4-CNB molecules rather than the TiO_2 particles since UV itself can directly decompose the 4-CNB (as can be seen form Fig. 6a).

The effect of catalyst dosage on degradation rate was studied by varying catalyst dosage from 0.1 to 1.0 g/L. The results are illustrated in Fig. 8. It is found that the degradation efficiency of 4-CNB increased significantly from 0.02293 to 0.1059 min^{-1} with increase of catalyst concentration at a range from 0.1 to 0.5 g/L and then increased much slowly with further increase of the catalyst concentration due to lights scattering and screening effect [37]. Many literature studies pointed out that the catalyst amount beyond 2.0 g/L will result in the deterioration of the degradation

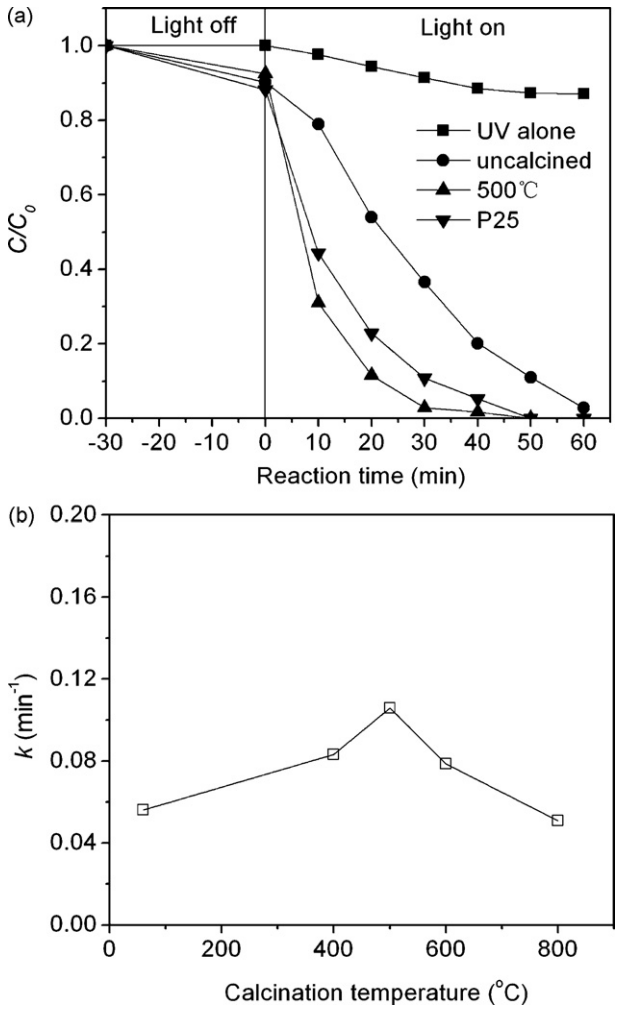

Fig. 6. (a) Photocatalytic degradation of 4-CNB and (b) effects of calcination temperature on apparent rate constants of the TiO_2 hollow microspheres. Experimental conditions: $C_0 = 1.0 \times 10^{-5}$ mol/L, [TiO_2] = 0.5 g/L, pH 6.8.

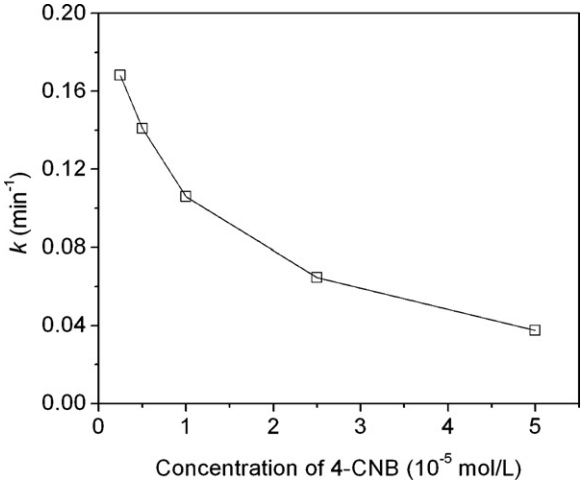

Fig. 7. Effect of 4-CNB concentration on the photodegradation rate of 4-CNB at $[TiO_2] = 0.5$ g/L, pH 6.8.

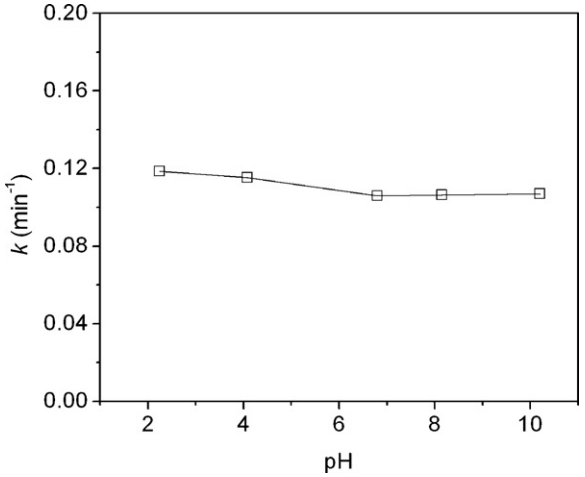

Fig. 9. Effect initial solution pH on the photodegradation rate of 4-CNB at $C_0 = 1.0 \times 10^{-5}$ mol/L, $[TiO_2] = 0.5$ g/L.

efficiency [38,39]. Therefore, 0.5 g/L was selected as the optimum concentration of catalyst in our experimental reaction system.

In order to realize the role of pH on the photocatalytic degradation rate, the initial solution pHs used for this study were adjusted at 2.24, 4.08, 6.80, 8.15 and 10.20 by adding sodium hydroxide or perchloric acid. As observed in Fig. 9, no significant differences are found in the 4-CNB removal efficiency within the tested reaction period of 60 min in different initial solution pH. However, the round neutral pH 6.8 shows a little bit lower performance than that of acidic or alkaline pH. In general, pH change will affect the zeta potential of catalyst. The zero point charge (zpc) pHzpc for TiO_2 is widely reported at about 6.5 [40–42]. At lower or higher than pHzpc, TiO_2 is positively or negatively charged, therefore the dispersiveness of the catalyst in solution is better than that in neutral condition, providing more reactive sites for adsorption and photocatalysis.

3.2.3. Mineralization of 4-CNB

The total organic carbon, chloride and nitrate (V) anions were monitored to obtain some useful information about the oxidation efficiency of the reactions and the mineralization of the 4-CNB. The results are shown in Fig. 10. It was found that the TOC removal rate was correspondingly lower than its concentration removal rate. More than 93% mineralization of the 4-CNB was reached at the irradiation time of 40 min whereas still 3% of the TOC was unremoved after the photocatalytic experiment finished, indicating the existence of byproducts in the reaction system. The uncompleted removal of TOC in each cycle is one of the reasons to explain why a small decrease in activity during catalyst reuse. The appearance of chloride and nitrate anions were observed from the early stages of the reaction, suggesting that chlorine atom and nitro group could be easily displaced by hydroxyl radicals (•OH) to form a variety of phenols [3,5]. The maximum concentrations of both chloride and nitrate anions were about 1.0×10^{-5} mol/L after reaction time of 60 min, respectively, showing a complete loss of chlorine atom and nitro group from 4-CNB.

3.2.4. Recycling

Microspheres have taken an advantage over powder catalysts for separating the catalyst from solution by filtration or sedimentation. In our experimental, the TiO_2 hollow microspheres can be separated from an aqueous suspension in less than 4 h by sedimentation, while the aqueous suspension of Degussa P25 was still turbid even after several days. Fig. 11 shows photodegradation of 4-CNB over the TiO_2 hollow microspheres calcined at 500 °C with 6-time cycling uses. It can be seen that the k value only decreased from 0.1059 to 0.9270 after six cycles, indicating that the photocatalysis had a good repeatability. There was no significant catalyst attrition happened during the photocatalysis because the concentration of Ti^{4+} in the solution was measured at 91.4 μg/L, which

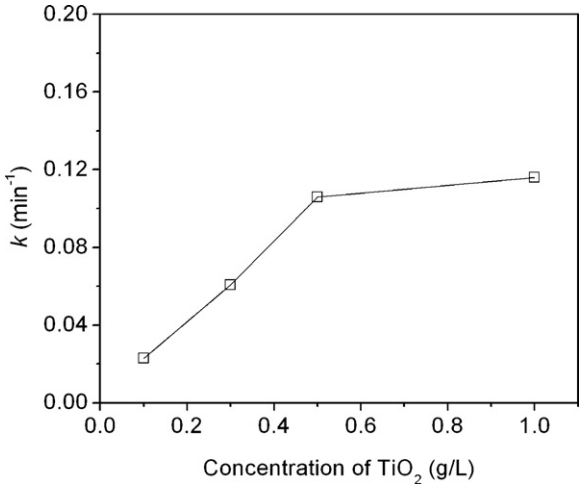

Fig. 8. Effect of catalyst dosage on the photodegradation rate of 4-CNB at $C_0 = 1.0 \times 10^{-5}$ mol/L, pH 6.8.

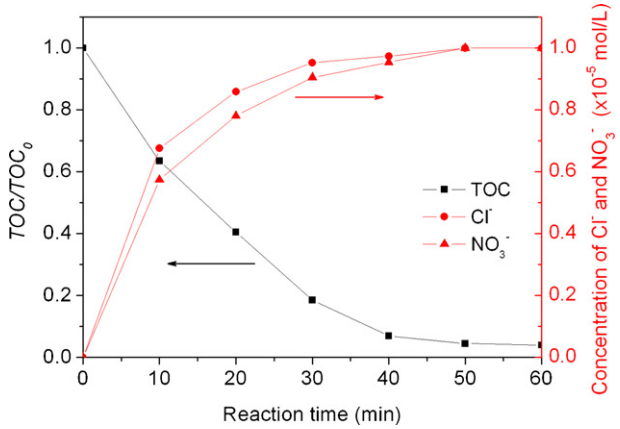

Fig. 10. TOC evolution and chloride, nitrate anions formations as a function of irradiation time. Experimental conditions: $C_0 = 1.0 \times 10^{-5}$ mol/L, $[TiO_2] = 0.5$ g/L, pH 6.8.

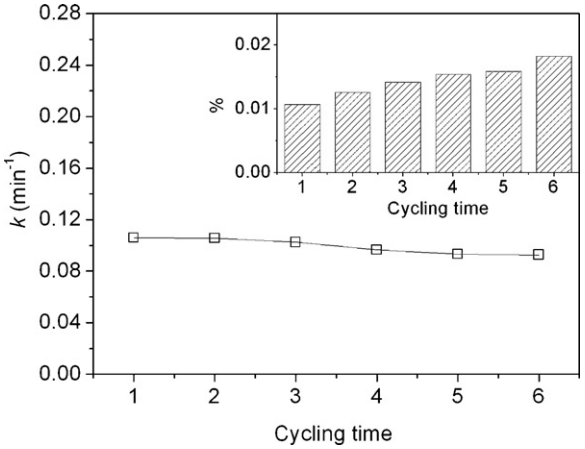

Fig. 11. Overall removal efficiency at reaction time of 60 min versus times of cycling uses for 4-CNB degradation. Inset: accumulated amount of Ti^{4+} dissolved in the solution after different cycles of photocatalysis.

was about only 0.018% of total TiO_2 in the system (out of a total of ca. 200 mg in 400 mL solution; inset of Fig. 11) even after 6 cycles. The slight decrease of degradation rate could be explained by the TiO_2 loss during sampling and filtration processes. The morphologies of the TiO_2 hollow microspheres calcined at 500 °C after 1-time and 6-time cycling uses were observed, respectively (as shown in Fig. 12). It can be seen from the pictures that no significant changes were happened even after 6-time cycling uses, which indicated that the chemical stability of the TiO_2 hollow microspheres was good. It may be one of the reasons to explain why these TiO_2 hollow microspheres exhibit good photocatalytic activity.

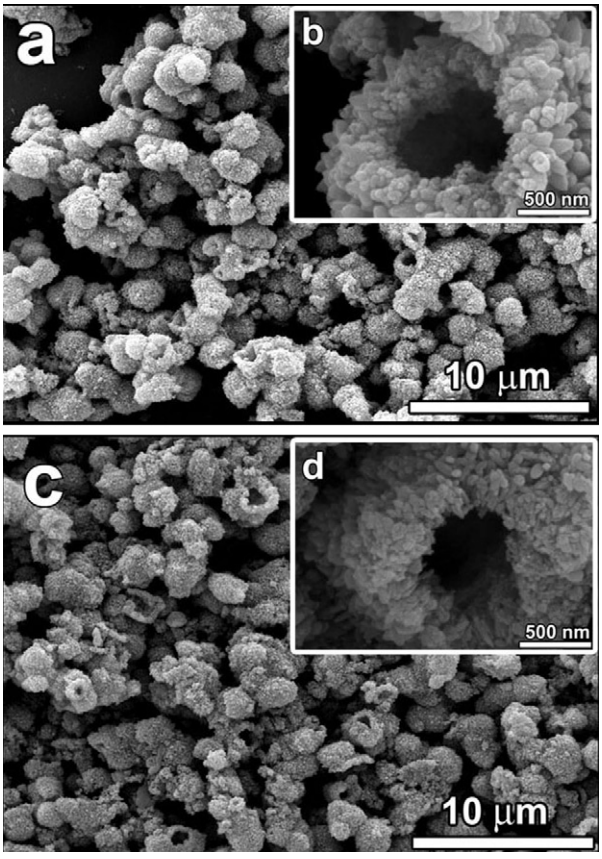

Fig. 12. SEM images of TiO_2 hollow microspheres calcined at 500 °C (a), (b) after 1-time use and (c), (d) after 6 times use.

4. Conclusions

In summary, TiO_2 hollow microspheres with an average external diameter of 1.75 μm were synthesized by means of a simple hydrothermal method. The shells of the hollow microspheres were composed of numerous nanoparticles. Calcination temperature exhibited a strong effect on the photocatalytic activity of the TiO_2 hollow microspheres. The TiO_2 hollow microspheres calcined at 500 °C showed the highest photocatalytic activity, which was about 2 and 1.5 times higher than that of the uncalcined sample and Degussa P25, respectively. The mineralization of 4-CNB by using the TiO_2 hollow spheres was efficient due to the special microstructure of the hollow microspheres, that is, the smaller crystal sizes, lager surface areas and pore volumes. Finally, it was demonstrated that these TiO_2 hollow microspheres could be recycled without decreasing its photocatalytic activity after 6-time cycling.

Acknowledgments

This work was supported financially by the Natural Science Foundation of China (Grant nos. 50638020 and 50821002), the National High Technology Research and Development Program of China (2007AA06Z339), Important National Science and Technology Specific Projects (2008ZX07421–003), to whom we are grateful. We also gratefully acknowledge Dr. Hu from University of California, Riverside for SEM and TEM measurements.

References

[1] G.S. Travlos, J. Mahler, H.A. Ragan, B.J. Chou, J.R. Bucheret, Thirteen-week inhalation toxicity of 2- and 4-chloronitrobenzene in F344/N Rats and B6C3F1 mice, Fundam. Appl. Toxicol. 30 (1996) 75–92.
[2] Z.B. Guo, S.R. Zheng, Z. Zheng, F. Jiang, W.Y. Hu, L.X. Ni, Selective adsorption of *p*-chloronitrobenzene from aqueous mixture of *p*-chloronitrobenzene and *o*-chloronitrobenzene using HZSM-5 zeolite, Water Res. 39 (2005) 1174–1192.
[3] M.M. Ye, Z.L. Chen, X.W. Liu, Y. Ben, J.M. Shen, Ozone enhanced activity of aqueous titanium dioxide suspensions for photodegradation of 4-chloronitrobenzene, J. Hazard. Mater. 167 (2009) 1021–1027.
[4] T. Yoshida, Determination of *p*-chloronitrobenzene and its metabolites in urine by reversed-phase high-performance liquid Chromatography, J. Chromatogr. 613 (1993) 79–88.
[5] J.M. Shen, Z.L. Chen, Z.Z. Xu, X.Y. Li, B.B. Xu, F. Qi, Kinetics and mechanism of degradation of *p*-chloronitrobenzene in water by ozonation, J. Hazard. Mater. 52 (2008) 1325–1331.
[6] J.P. Ge, T. Huynh, Y.X. Hu, Y.D. Yin, Hierarchical magnetite/silica nanoassemblies as magnetically recoverable catalyst-supports, Nano Lett. 8 (2008) 931–934.
[7] I.K. Konstantinou, T.A. Albanis, TiO_2-assisted photocatalytic degradation of azo dyes in aqueous solution: kinetic and mechanistic investigations: a review, Appl. Catal. B: Environ. 49 (2004) 1–14.
[8] A. Houas, H. Lachheb, M. Ksibi, E. Elaloui, C. Guillard, J.M. Herrmann, Photocatalytic degradation pathway of methylene blue in water, Appl. Catal. B: Environ. 31 (2001) 145–157.
[9] Z.D. Lu, M.M. Ye, N. Li, W.W. Zhong, Y.D. Yin, Self-assembled TiO_2 nanocrystal clusters for selective enrichment of intact phosphorylated proteins, Angew. Chem. Int. Ed. 49 (2010) 1862–1866.
[10] M.M. Ye, Z.L. Chen, W.S. Wang, L. Zhen, J.M. Shen, Large-scale synthesis and characterization of fan-shaped rutile TiO_2 nanostructures, Mater. Lett. 62 (2008) 3404–3406.
[11] A. Rachel, M. Subrahmnyam, P. Boule, Comparison of photocatalytic efficiencies of TiO_2 in suspended and immobilised form for the photocatalytic degradation of nitrobenzenesulfonic acids, Appl. Catal. B: Environ. 37 (2002) 301–308.
[12] A. Haarstrick, O.M. Kut, E. Heinzle, TiO_2-assisted degradation of environmentally relevant organic compounds in wastewater using a novel fluidized bed photoreactor, Environ. Sci. Technol. 30 (1996) 817–824.
[13] B.L. Zhang, B.S. Chen, K.Y. Shi, S.J. He, X.D. Liu, Z.J. Du, K.L. Yang, Preparation and characterization of nanocrystal grain TiO_2 porous microspheres, Appl. Catal. B: Environ. 40 (2003) 253–258.
[14] X.Z. Li, H. Liu, L.F. Cheng, H.J. Tong, Photocatalytic oxidation using a new catalyst-TiO_2 microsphere for water and wastewater treatment, Environ. Sci. Technol. 37 (2003) 3989–3994.
[15] T. Nakashima, N. Kimizuka, Interfacial synthesis of hollow TiO_2 microspheres in ionic liquids, J. Am. Chem. Soc. 125 (2003) 6386–6387.
[16] J.G. Yu, H.T. Guo, S.A. Davis, S. Mann, Fabrication of hollow inorganic microspheres by chemically induced self-transformation, Adv. Funct. Mater. 16 (2006) 2035–2041.

[17] Y.Z. Li, T. Kunitake, S. Fujikawa, Efficient fabrication and enhanced photocatalytic activities of 3D-ordered films of titania hollow spheres, J. Phys. Chem. B 110 (2006) 13000–13004.
[18] Y.H. Ao, J.J. Xu, D.G. Fu, C.W. Yuan, A simple method for the preparation of titania hollow sphere, Catal. Commum. 9 (2008) 2574–2577.
[19] M.M. Ye, Z.L. Chen, W.S. Wang, L. Zhen, J.M. Shen, Template-free hydrothermal preparation of mesoporous TiO_2 microspheres on a large scale, Chem. Lett. 37 (2008) 938–939.
[20] Z.Y. Liu, D.D. Sun, P. Guo, J.O. leckie, One-step fabrication and high photocatalytic activity of porous TiO_2 hollow aggregates by using a low-temperature hydrothermal method without templates, Chem. Eur. J. 13 (2007) 1851–1855.
[21] H.X. Li, Z.F. Bian, J. Zhu, D.Q. Zhang, G.S. Li, Y.N. Huo, H. Li, Y.F. Lu, Mesoporous titania spheres with tunable chamber stucture and enhanced photocatalytic activity, J. Am. Chem. Soc. 129 (2007) 8406–8407.
[22] J.G. Yu, W. Liu, H.G. Yu, A one-pot approach to hierarchically nanoporous titania hollow microspheres with high photocatalytic activity, Cryst. Growth Des. 8 (2008) 930–934.
[23] X.X. Li, Y.J. Xiong, Z.Q. Li, Y. Xie, Large-scale fabrication of TiO_2 hierarchical hollow spheres, Inorg. Chem. 45 (2006) 3493–3495.
[24] H. Wang, Y. Wu, B.Q. Xu, Preparation and characterization of nanosized anatase TiO_2 cuboids for photocatalysis, Appl. Catal. B: Environ. 59 (2005) 139–146.
[25] K.S.W. Sing, D.H. Everett, R.A.W. Haul, L. Moscou, R.A. Pierotti, J. Rouquerol, T. Siemieniewska, Reporting physisorting physisorption data for gas/solid systems with special reference to the determination of surface area and porosity, Pure Appl. Chem. 57 (1985) 603–619.
[26] Y.J. Chen, D.D. Dionysiou, Bimodal mesoporous TiO_2–P25 composite thick films with high photocatalytic activity and improved structural integrity, Appl. Catal. B: Environ. 80 (2008) 147–155.
[27] Y.J. Chen, D.D. Dionysiou, A comparative study on physicochemical properties and photocatalytic behavior of macroporous TiO_2–P25 composite films and macroporous TiO_2 films coated on stainless steel substrate, Appl. Catal. A: Gen. 317 (2007) 129–137.
[28] Y.J. Chen, D.D. Dionysiou, Correlation of structural properties and film thickness to photocatalytic activity of thick TiO_2 films coated on stainless steel, Appl. Catal. B: Environ. 69 (2006) 24–33.
[29] J.G. Yu, M.H. Zhou, B. Cheng, X.J. Zhao, Preparation, characterization and photocatalytic activity of in situ N,S-codoped TiO_2 powders, J. Mol. Catal. A: Chem. 246 (2006) 176–184.
[30] J.G. Yu, G.H. Wang, B. Cheng, M.H. Zhou, Effects of hydrothermal temperature and time on the photocatalytic activity and microstructures of bimodal mesoporous TiO_2 powders, Appl. Catal. B: Environ. 69 (2007) 171–180.
[31] N. Serpone, D. Lawless, R. Khairutdinov, Size effects on the photophysical properties of colloidal anatase TiO_2 particles: size quantization ordirect transitions in this indirect semiconductor, J. Phys. Chem. 99 (1995) 16646–16654.
[32] K.M. Reddy, S.V. Manorama, A.R. Reddy, Bandgap studies on anatase titanium dioxide nanoparticles, Mater. Chem. Phys. 78 (2002) 239–245.
[33] Y.X. Zhang, G.H. Li, Y.C. Wu, Y.Y. Luo, L.D. Zhang, The formation of mesoporous TiO_2 spheres via a facile chemical process, J. Phys. Chem. B. 109 (2005) 5478–5484.
[34] Y.J. Chen, D.D. Dionysiou, Effect of calcination temperature on the photocatalytic activity and adhesion of TiO_2 films prepared by the P-25 powder-modified sol–gel method, J. Mol. Catal. A: Chem. 244 (2006) 73–82.
[35] Z.Y. Liu, X. Quan, H.B. Fu, X.Y. Li, K. Yang, Effect of embedded-silica on microstructure and photocatalytic activity of titania prepared by ultrasound-assisted hydrolysis, Appl. Catal. B: Environ. 52 (2004) 33–40.
[36] J.G. Yu, J.C. Yu, M.K.P. Leung, W.K. Ho, B. Cheng, X.J. Zhao, J.C. Zhao, Effects of acidic and basic hydrolysis catalysts on the photocatalytic activity and microstructures of bimodal mesoporous titania, J. Catal. 217 (2003) 69–78.
[37] C.M. Zhu, L.Y. Wang, L.R. Kong, X. Yang, L.S. Wang, S.J. Zheng, F.L. Chen, F.M. Zhi, H. Zong, Photocatalytic degradation of AZO dyes by supported TiO_2 + UV in aqueous solution, Chemosphere 41 (2000) 303–309.
[38] M.V. Shankar, K.K. Cheralathan, B. Arabindoo, M. Palanichamy, V. Murugesan, Enhanced photocatalytic activity for the destruction of monocrotophos pesticide by TiO_2/Hβ, J. Mol. Catal. A: Chem. 223 (2004) 195–200.
[39] T.Y. Wei, C.C. Wan, Heterogeneous photocatalytic oxidation of phenol with titanium dioxide powders, Ind. Eng. Chem. Res. 30 (1991) 1293–1300.
[40] C. Kormann, D.W. Bahnemann, M.R. Hoffmann, Photolysis of chloroform and other organic molecules in aqueous TiO_2 suspensions, Environ. Sci. Technol. 25 (1991) 494–500.
[41] P.O. Vasiliev, B. Faure, J.B.S. Ng, L. Bergstrom, Colloidal aspects relating to direct incorporation of TiO_2 nanoparticles into mesoporous spheres by an aerosol-assisted process, J. Colloid Interface Sci. 319 (2008) 144–151.
[42] R. Greenwood, Review of the measurement of zeta potentials in concentrated aqueous suspensions using electroacoustics, Adv. Colloid Interface Sci. 106 (2003) 55–81.